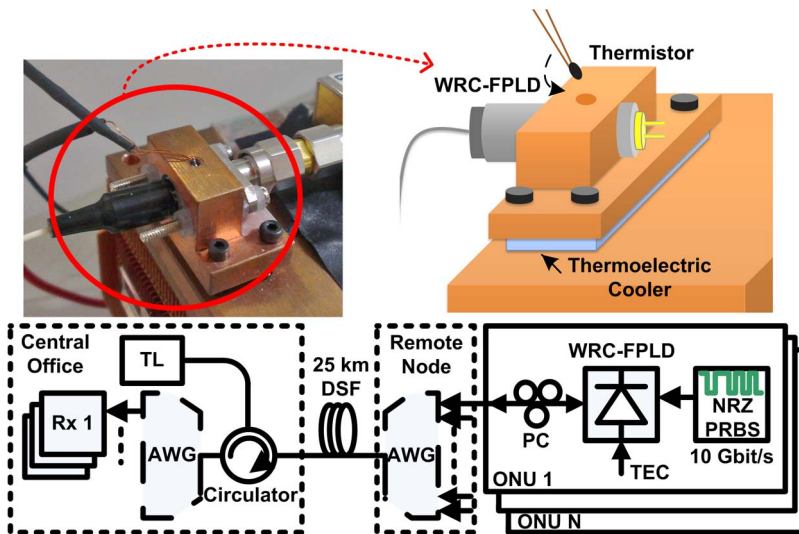


# An Injection-Locked Weak-Resonant-Cavity Laser Diode for Beyond-Bandwidth Encoded 10-Gb/s OOK Transmission

Volume 7, Number 1, February 2015

Shih-Ying Lin  
Yu-Chieh Chi  
Yu-Chuan Su  
Yi-Cheng Li  
Gong-Ru Lin



---

DOI: 10.1109/JPHOT.2015.2395135  
1943-0655 © 2015 IEEE

# An Injection-Locked Weak-Resonant-Cavity Laser Diode for Beyond-Bandwidth Encoded 10-Gb/s OOK Transmission

Shih-Ying Lin, Yu-Chieh Chi, Yu-Chuan Su, Yi-Cheng Li, and Gong-Ru Lin

Graduate Institute of Photonics and Optoelectronics and the Department of Electrical Engineering,  
National Taiwan University, Taipei 10617, Taiwan

DOI: 10.1109/JPHOT.2015.2395135

1943-0655 © 2015 IEEE. Translations and content mining are permitted for academic research only.  
Personal use is also permitted, but republication/redistribution requires IEEE permission.  
See [http://www.ieee.org/publications\\_standards/publications/rights/index.html](http://www.ieee.org/publications_standards/publications/rights/index.html) for more information.

Manuscript received November 24, 2014; revised January 8, 2015; accepted January 17, 2015. Date of publication January 23, 2015; date of current version February 10, 2015. This work was supported by the Taiwanese Ministry of Science and Technology under Grant NSC 101-2221-E-002-071-MY3, Grant MOST 103-2221-E-002-042-MY3, and Grant MOST 103-2218-E-002-017-MY3. Corresponding author: G.-R. Lin (e-mail: grlin@ntu.edu.tw).

**Abstract:** A coherently injection-locked and beyond-bandwidth-modulated weak-resonant-cavity laser diode (WRC-FPLD) transmitter packaged by a conventional TO-56 can package for an upstream 10-Gb/s OOK transmission is demonstrated in a DWDM-PON. With specific temperature controlling, the WRC-FPLD is able to maintain its temperature during the process of injection locking. Based on the theoretical analysis of modified rate equations, the injection-locked WRC-FPLD exhibits not only a broadband gain spectrum but also a large modulation bandwidth. Successfully implementing injection locking enhances the high-frequency throughput response but inevitably impairs the throughput intensity at a low-frequency region. By properly increasing the injection-locking power, the modulation bandwidth of the injection-locked WRC-FPLD can be further improved. In addition, the extinction ratio and the signal-to-noise ratio (SNR) of the transmitted 10-Gb/s NRZ-OOK data can also be improved from 5.58 to 6.95 dB and from 5.43 to 6.18, respectively, by increasing the injection-locking power from  $-12$  to  $-3$  dBm, which improves the receiving power sensitivity by 1.6 dB. The optimized receiving power sensitivity at a requested bit error rate (BER) of  $10^{-9}$  is  $-15.4$  dBm by setting the injection-locking power at  $-3$  dBm. After a 25-km transmission, such an overbandwidth-modulated and injection-locked WRC-FPLD reveals a receiving power sensitivity of  $-11.6$  dBm at the same BER of  $10^{-9}$ .

**Index Terms:** Beyond bandwidth modulation, conventional TO-56-can package, weak-resonant-cavity laser diode, injection locking.

## 1. Introduction

The dense wavelength division multiplexed passive optical network (DWDM-PON) has been recognized as an ultimate solution for next-generation broadband access network [1], [2] owing to its high transmission capacity. For developing a practical DWDM-PON, the colorless laser transmitters such as the reflective semiconductor optical amplifiers (RSOAs) [3], [4], the amplified spontaneous emission (ASE) injected Fabry–Perot laser diodes (FPLDs) [5], the mutually injection-locked FPLDs [6], and the weak-resonant-cavity FPLDs (WRC-FPLDs) [7], [8] have been demonstrated. The universal laser transmitter with broadband gain spectrum is able to provide each DWDM channel its own carrier wavelength [9]. Therefore, it is important for laser

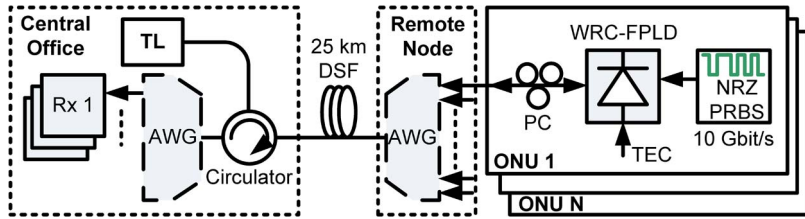


Fig. 1. DWDM-PON testing system with coherently injection locked and directly modulated WRC-FPLDs as the up-stream ONU transmitters.

transmitters to possess the advantage of colorless operation and large transmission capacity in bringing DWDM-PON into practice. In previous works, there were several attempts to operate the broadband laser transmitters at up to 10 Gbit/s in DWDM-PON system. A continuous wave (CW) injection-locked FPLD based bidirectional transmission was presented in 2007 [10], which demonstrated the possibility of offering 16 channels for DWDM-PON application. In 2008, by using the directly modulated RSOAs combined with the electronic equalizers, a 10-Gbit/s DWDM-PON has been demonstrated [11], [12]. However, the transmission performance is inevitably limited by the modulation bandwidth of RSOAs, which is only about 2 GHz. To make a balance between the broadness of gain spectrum and the coherence of throughput light, the WRC-FPLD was proposed in 2009. Such a new class of laser transmitter was originated from the imperfect anti-reflection (AR) coating on the front-facet of a long-cavity FPLD. By lowering the front-facet reflectance and increasing the cavity length, the WRC-FPLD shows broader gain spectrum than the conventional FPLD and better coherence with lower noise figure than the RSOA. In previous years, the ASE-injected WRC-FPLD based DWDM-PON with 1.25-Gbit/s transmission data rate was proposed [13], and many operating characteristics such as the bias current and the injected mode number [8] have been discussed in detail. By replacing the injection source from ASE to tunable laser, the data rate of the injection-locked WRC-FPLD transmitter can be upgraded to 2.5 Gbit/s [14]. As the WRC-FPLD possesses both properties of broad gain spectrum and partial coherence, it is worthy to investigate the possibility of operating the injection-locked WRC-FPLD transmitter for high-speed nonreturn-to-zero on-off-keying (NRZ-OOK) modulation. Besides, the injection locking is a pivotal technique in using colorless laser transmitters for selecting specific wavelength for each optical network unit (ONU) in DWDM-PON. In fact, the injection locking properties of semiconductor lasers have been widely discussed to enhance the modulation bandwidth [15]–[17] and suppress the frequency chirp [18], [19].

In this work, a coherently injection-locked WRC-FPLD packaged by a conventional TO-56-can package is demonstrated as the 10-Gbit/s transmitter in DWDM-PON system. To further understand the effect of injection-locking power on output dynamics of the injection-locked WRC-FPLD, the modified rate equations are also discussed. In addition, the modulation bandwidth, eye-diagram, and bit-error-rate (BER) performances of the injection-locked WRC-FPLD under 10-Gbit/s NRZ-OOK data modulation are characterized. In consideration of practical optical distribution network, the 25-km 10-Gbit/s NRZ-OOK data transmission is also represented.

## 2. Experimental Setup

A DWDM-PON system with coherently injection-locked and directly modulated WRC-FPLD transmitters for transmitting the 10-Gbit/s NRZ-OOK data is illustrated in Fig. 1. A rear-facet high-reflective coating with reflectance of 93% and a front-facet low-reflective coating with reflectance of 1.2% were employed for the slave WRC-FPLD with a cavity length of  $600\ \mu\text{m}$ . In DWDM-PON, the colorless WRC-FPLD packaged by a conventional TO-56-can package was used as a universal transmitter owing to its advantage of broadband gain spectrum and was injection locked by a tunable laser (ANDO, AQ4321D) passing through an optical circulator. The original wavelength of selected mode for the slave WRC-FPLD to be injection locked is 1569.23 nm, and the injected master wavelength of 1569.38 nm was slightly red-shifted by

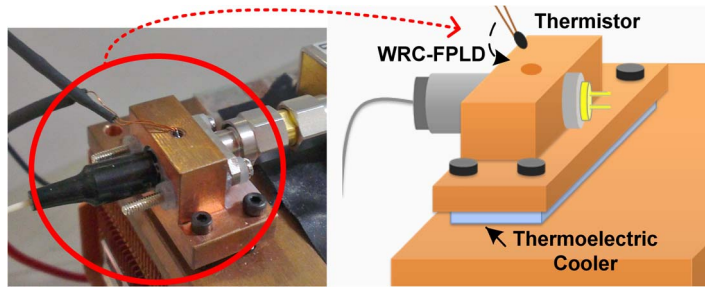


Fig. 2. WRC-FPLD with temperature controlling.

0.15 nm to optimize the injection-locking performance [20]. A wideband bias-tee (Mini-circuits, ZX85-12G-S+) was used to couple the DC bias and the modulating data for driving the WRC-FPLD. The WRC-FPLD was directly modulated by a 10-Gbit/s NRZ-OOK data generated from a pattern generator (Agilent, 70843B) with a pattern length of  $2^{23} - 1$ . The operating DC bias was set at two times of the threshold current ( $I_{th}$ ) and the peak-to-peak amplitude of the electrical 10-Gbit/s NRZ-OOK data was set at 1.3 V.

The eye-diagram of the optical 10-Gbit/s NRZ-OOK data transmitted by the injection-locked WRC-FPLD was analyzed by a digital sampling oscilloscope (Agilent, 86106A). In addition, the BER performance of the injection-locked WRC-FPLD carried 10-Gbit/s NRZ-OOK data was analyzed via a commercial BER tester (Agilent, 70843A) after receiving with a standard Lightwave Receiver (Agilent 83434A) at bit rate of 10 Gbit/s. A dispersion-shifted fiber (DSF, Corning MetroCore Optical Fiber) was inserted into DWDM-PON system to investigate the 25-km transmission performance of the injection-locked WRC-FPLD delivered high-speed data. To avoid the fluctuation of temperature affecting the stability of injection locking, a specific copper mount was designed for the conventional TO-56-can packaged WRC-FPLD, as shown in Fig. 2. Such a mount was made by copper owing to its characteristic of high thermal conductivity. To further avoid the copper mount affecting the laser frequency response, the WRC-FPLD was insulated from touching the copper. Finally, the thermistor and the thermoelectric cooler were controlled by a modular laser diode controller (ILX Lightwave, LDC-3900) to maintain the temperature of the WRC-FPLD at 23.5 °C.

### 3. Results and Discussions

#### 3.1. Modeling

By adopting the theoretical model proposed for a single-wavelength FPLD under external injection locking [17], the rate equations can be described as follows:

$$\frac{dN(t)}{dt} = \frac{\eta_i I}{qV} - \frac{N(t)}{\tau_s} - v_g g' [N(t) - N_{tr}] S(t) \quad (1)$$

$$\frac{d\phi(t)}{dt} = \frac{1}{2} \alpha \Gamma v_g g' [N(t) - N_{tr}] - \kappa \sqrt{\frac{S_{inj}}{S_B}} \sin(\Delta\phi(t)) - \Delta\omega_{inj} \quad (2)$$

$$\frac{dS(t)}{dt} = \Gamma v_g g' [N(t) - N_{tr}] S(t) - \frac{S(t)}{\tau_p} + 2\kappa \sqrt{S_{inj} S(t)} \cos(\Delta\phi(t)) \quad (3)$$

where  $N$  denotes the carrier density,  $\phi$  the phase,  $S$  the photon density of the slave laser diode,  $\eta_i$  the internal quantum efficiency,  $I$  the bias current,  $q$  the quantum charge,  $V$  the volume,  $\tau_s$  the spontaneous carrier lifetime,  $v_g$  the velocity,  $g'$  the differential gain,  $N_{tr}$  the transparent carrier density,  $\alpha$  the linewidth enhancement factor,  $\Gamma$  the optical confinement factor,  $\kappa$  the coupling efficiency,  $S_{inj}$  the injection photon density,  $S_B$  the average output photon density,  $\Delta\phi$  the phase difference between master and slave lasers ( $\Delta\phi \equiv \phi_{slave} - \phi_{master}$ ),  $\Delta\omega_{inj}$  the detuning frequency,

and  $\tau_p$  the photon lifetime. Therein, the detuning frequency is defined as the angular frequency difference between the master and the slaver lasers, which refers to the wavelength difference between two lasers. By considering the injection-locking term  $S_{\text{inj}}$ , the additional coupling of photon density to the phase enhances the relaxation oscillation frequency and the damping rate of the injection-locked laser diode [21], [22]. Therefore, (2) must be considered in analysis for an injection-locked semiconductor laser diode. The small-signal modulation response of an injection-locked laser diode can be analyzed by assuming that the dynamic changes in carrier and photon densities away from their steady-state values are small. Then, the differential rate equations can be described in a compact matrix form as

$$\begin{bmatrix} \gamma_{11} + j\omega & \gamma_{12} & \gamma_{13} \\ \gamma_{21} & \gamma_{22} + j\omega & \gamma_{23} \\ \gamma_{31} & \gamma_{32} & \gamma_{33} + j\omega \end{bmatrix} \begin{bmatrix} N_1(\omega) \\ \phi_1(\omega) \\ S_1(\omega) \end{bmatrix} = \frac{\eta_i}{qV} \begin{bmatrix} I_1(\omega) \\ 0 \\ 0 \end{bmatrix} \quad (4)$$

where

$$\begin{aligned} \gamma_{11} &= \frac{1}{\tau_s} + v_g g' S_B, & \gamma_{12} &= 0, & \gamma_{13} &= \frac{1}{\Gamma \tau_p} - \frac{2\kappa}{\Gamma} \sqrt{\frac{S_{\text{inj}}}{S_B}} \cos(\phi_B - \phi_i) - v_g a_p S_B \\ \gamma_{21} &= -\frac{1}{2} \alpha \Gamma v_g g', & \gamma_{22} &= \kappa \sqrt{\frac{S_{\text{inj}}}{S_B}} \cos(\phi_B - \phi_i), & \gamma_{23} &= \frac{1}{2} \alpha \Gamma v_g a_p - \frac{1}{2} \kappa \sqrt{\frac{S_{\text{inj}}}{S_B^3}} \sin(\phi_B - \phi_i) \\ \gamma_{31} &= -\Gamma v_g g' S_B, & \gamma_{32} &= 2\kappa \sqrt{S_{\text{inj}} S_B} \sin(\phi_B - \phi_i), & \gamma_{33} &= \Gamma v_g S_B a_p + \kappa \sqrt{\frac{S_{\text{inj}}}{S_B}} \cos(\phi_B - \phi_i). \end{aligned} \quad (5)$$

By applying Cramer's rule, the relation between photon density and DC bias can be obtained. Then, the magnitude frequency response can be described as

$$H(\omega) = \frac{\frac{\eta_i}{qV} [Dj\omega + E]}{-j\omega^3 + A\omega^2 + Bj\omega + C} \quad (6)$$

where

$$\begin{aligned} A &= -(\gamma_{11} + \gamma_{22} + \gamma_{33}) \\ B &= \gamma_{11}\gamma_{22} + \gamma_{11}\gamma_{33} + \gamma_{22}\gamma_{33} - \gamma_{23}\gamma_{32} - \gamma_{13}\gamma_{31} \\ C &= \gamma_{11}\gamma_{22}\gamma_{33} - \gamma_{11}\gamma_{32}\gamma_{23} + \gamma_{13}\gamma_{21}\gamma_{32} - \gamma_{13}\gamma_{31}\gamma_{22} \\ D &= -\gamma_{31} \\ E &= \gamma_{21}\gamma_{32} - \gamma_{31}\gamma_{22}. \end{aligned} \quad (7)$$

The small-signal modulation response can further be simulated by using a home-made MATLAB program. The requested characteristic parameters of the injection-locked WRC-FPLD for analytically solving the aforementioned equations are summarized in Table 1. Therein, the correlation between mirror loss ( $\alpha_m$ ) and reflectances is defined as  $\alpha_m = (1/2L)\ln(1/R_f R_b)$  [23], where  $L$  denotes the cavity length,  $R_f$  the front facet reflectance, and  $R_b$  the rear facet reflectance.

Based on the (6), the simulated modulation responses of the free-running WRC-FPLD with different front-facet reflectances at bias current of  $2I_{\text{th}}$  and  $3I_{\text{th}}$  are shown in Fig. 3, respectively. During the simulation, we do not observe the non-stable locking phenomenon as most of operating parameters were properly set at optimized injection-locking condition. The WRC-FPLD with lower front-facet reflectance shows larger threshold carrier density than a typical FPLD.

Therefore, with the same ratio of the bias current over the threshold current, the WRC-FPLD with lower front-facet reflectance leads to larger 3-dB modulation bandwidth. Besides, according to the relation that  $f_{3\text{dB}}$  is proportional to  $(I_{\text{bias}} - I_{\text{th}})^{0.5}$ , the modulation bandwidth can be significantly enhanced by increasing the bias current, which is equivalent to our simulation results. Furthermore, the bandwidth variation between different front-facet reflectances is much apparent at high bias current condition. In general, the WRC-FPLD with low front-facet reflectance possesses not only broadband gain spectrum but large modulation bandwidth under the same bias current ratio ( $I_{\text{bias}}/I_{\text{th}}$ ) operation as well.

TABLE 1

The parameters of the injection-locked WRC-FPLD transmitter for the modified rate equations simulation

	WRC-FPLD			
Active layer thickness ( $\mu\text{m}$ )	0.008			
Cavity length ( $\mu\text{m}$ )	600			
Active layer width ( $\mu\text{m}$ )	1.5			
Rear Facet Reflectance	93%			
Carrier number at transparency	7.29E7			
Carrier lifetime (ns)	1			
Optical confinement factor	0.032			
Group velocity (cm/s)	0.857E10			
Internal loss ( $\text{cm}^{-1}$ )	30			
Front Facet Reflectance (%)	0.1	1	10	30
Mirror loss ( $\text{cm}^{-1}$ )	58.17	38.98	19.79	10.63
Threshold Gain ( $\text{cm}^{-1}$ )	2755.3	2155.7	1556	1269.93
Carrier number at threshold	1.28E8	1.16E8	1.04E8	0.98E8
Photon lifetime (ps)	1.32	1.69	2.3	2.87

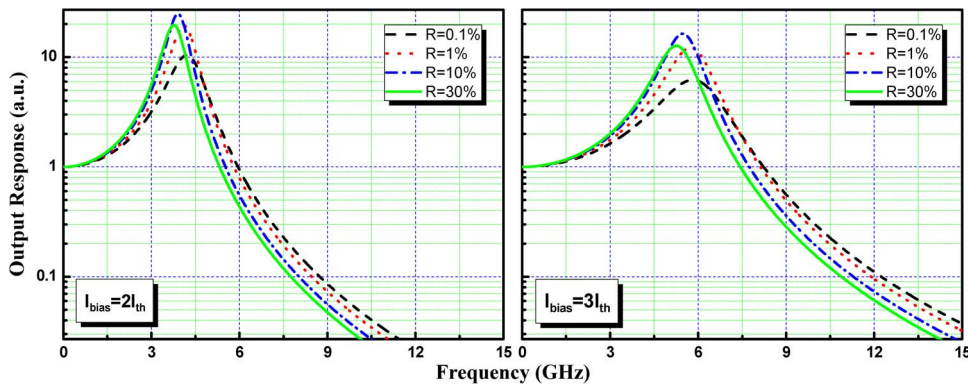


Fig. 3. Simulated modulation responses of the WRC-FPLD with different front-facet reflectances at bias current of  $2I_{\text{th}}$  (left) and  $3I_{\text{th}}$  (right).

The simulated frequency responses of the WRC-FPLD under injection locking are shown in Fig. 4. By increasing the injection-locking power, the modulation bandwidth and the throughput intensity of the injection-locked WRC-FPLD can be improved. In addition, the relaxation oscillation frequency of the injection-locked WRC-FPLD can be slightly enhanced due to the enhancement on both the relative strength of the coupling and gain coefficients. However, as the injection power goes to 6 dBm or 9 dBm, such a high injection power level degrades the throughput response instead of improving the modulation bandwidth. The over-injected and unmodulated photons are unable to create more stimulated emitting photons but become noise component in the slave laser cavity. Nevertheless, the critical value of injection power is dependent on many parameters, such as the front-facet reflectance, the cavity length, etc. According to our simulation results, the critical value of injection power increases as the front-facet reflectance is enlarged because of the enhanced cavity effect. The WRC-FPLD with larger front-facet reflectance possesses smaller damping coefficient, thus requiring higher injection level to stabilize the single-mode output performance.

### 3.2. Measured Output Dynamics of the Injection-Locked and Directly Modulated WRC-FPLD

The measured frequency response without any dip for the WRC-FPLD under free-running operation exhibits its flatness at frequency below 5 GHz, as shown in Fig. 5, which proves that the copper mount does not impair the frequency response of the WFC-FPLD. In view of

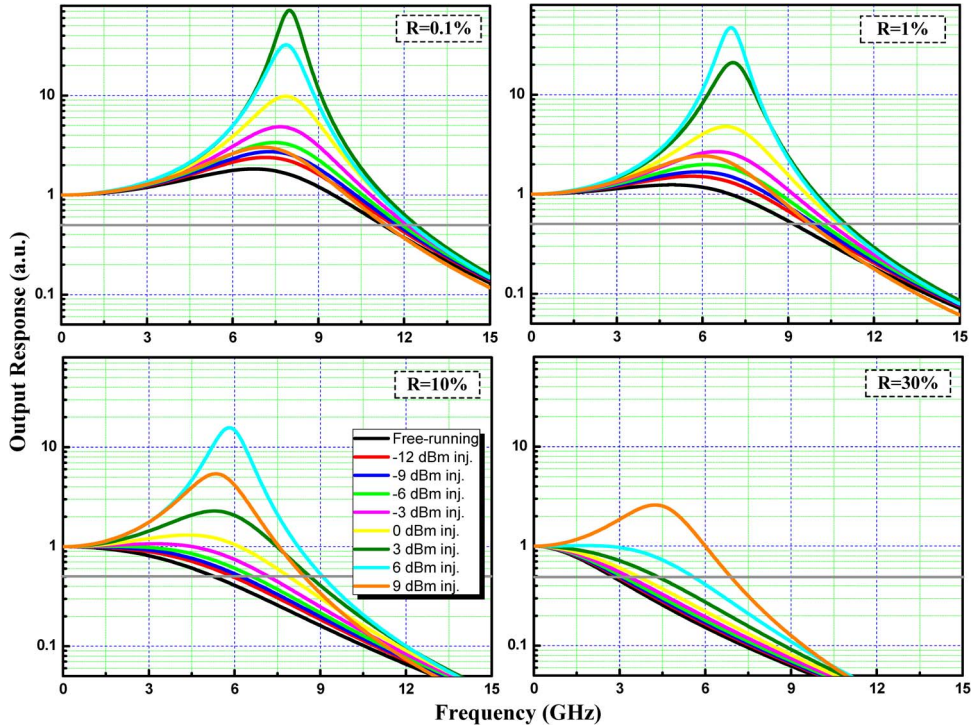


Fig. 4. Theoretical simulation of the small-signal modulation response for the injection locked WRC-FPLD.

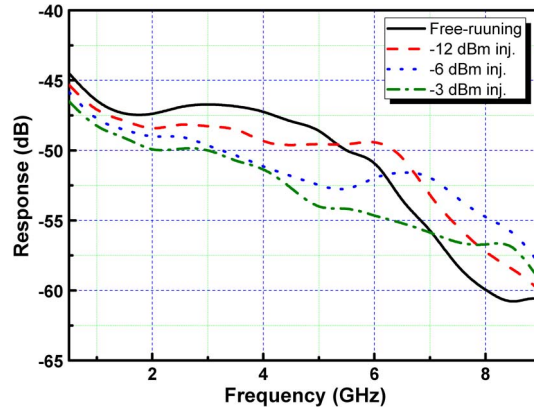


Fig. 5. Measured frequency response of the WRC-FPLD without and with injection locking.

previous reports, we understand that the chaos of an injection-locked laser diode usually occurs when the detuning frequency and the injection ratio are incorrectly assigned within the unstable region [24]–[26]. In experiment, although the chaos occasionally appears, this phenomenon is minimized by precisely detuning the parameters so as to operate the WRC-FPLD normally. With an injection power of  $-12$  dBm, the relaxation oscillation frequency of the WRC-FPLD is slightly enhanced, which is attributed to the enhancement on both the relative strength of the coupling and gain coefficients [22]. With increasing the injection power, the throughput response at low frequency region inevitably decreases. Nevertheless, the improved response at high frequency region promotes the high-speed transmission performance. The measured small-signal modulation response reveals a similar trend with the simulated one; however, the real frequency

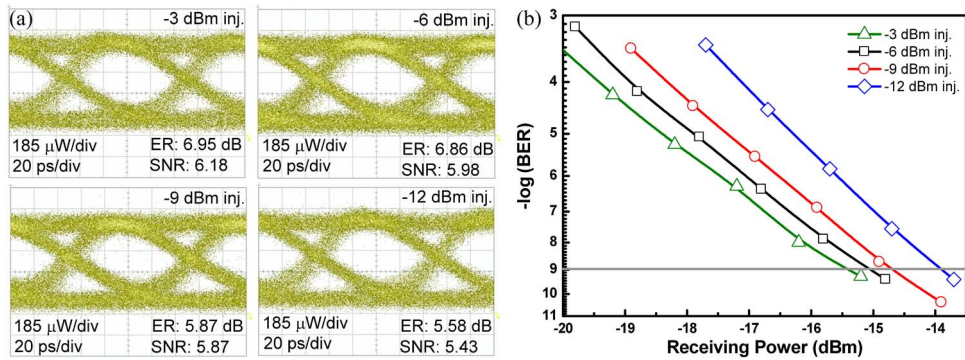


Fig. 6. Eye-diagrams (left) and BER (right) of the directly modulated and injection locked WRC-FPLD delivered 10-Gbit/s NRZ-OOK data at different injection powers.

response of the WRC-FPLD is concurrently limited by the TO-56-can package with inherent parasitic capacitance and inductance. This will induce a deviation between the experimental results and the ideal simulation without considering the package.

The Fig. 6 shows the back-to-back 10-Gbit/s NRZ-OOK data transmission performance of the directly modulated and injection-locked WRC-FPLD at different injection powers. The bias current of the WRC-FPLD is properly adjusted to obtain the highest extinction ratio (ER). With an injection power of  $-12\text{ dBm}$ , the directly modulated WRC-FPLD shows an acceptable eye-diagram with an ER of  $5.58\text{ dB}$  and a signal-to-noise ratio (SNR) of  $5.43$  representing a Q parameter of  $5.84$ . By enlarging the injection power from  $-12$  to  $-3\text{ dBm}$ , the ER and SNR can be improved by  $1.3\text{ dB}$  and  $0.7$ , respectively, because the increased injection power can further suppress the side-mode intensity and improve the high-frequency response. To discuss the transmission performance, the power penalty of  $-0.8\text{ dB}$  is observed for the injection-locked WRC-FPLD transmitted 10-Gbit/s NRZ-OOK data by increasing the injection power  $-12$  to  $-9\text{ dBm}$ . By further increasing the injection power to  $-6\text{ dBm}$ , the externally injected photons seem almost comparable with the excited carrier number inside the WRC-FPLD cavity. The overly injected photon number is less contributed to create more stimulated emitting photons. Therefore, as the injection power is larger than  $-9\text{ dBm}$ , the reduced power penalty is only around  $-0.3\text{ dB}$  with injection power increased by every  $3\text{ dB}$ . The 10-Gbit/s NRZ-OOK data is detectable at  $-15.4\text{ dBm}$  for meeting a requested BER of  $10^{-9}$  at an injection power of  $-3\text{ dBm}$ .

In consideration of a practical optical distribution network, the 25-km transmission performance of the injection-locked WRC-FPLD at a bit rate of 10 Gbit/s is discussed. The DSF which is able to shift the zero-dispersion wavelength to  $1550\text{ nm}$  allows the long-distant transmission with low dispersion and low attenuation. Therefore, the DSF is applied to suppress the chromatic dispersion for improving the 25-km transmission performance. The measured eye-diagrams of the directly modulated and injection-locked WRC-FPLD output after 25-km DSF transmission are shown in Fig. 7(a). The output eye-diagram of the injection locked WRC-FPLD at an injection power of  $-12\text{ dBm}$  shows the longest rising time of  $42.2\text{ ps}$ . When the injection power is enlarged to  $-9\text{ dBm}$ , the rising time can be shorted to  $34.7\text{ ps}$  owing to the improved modulation response. However, as the throughput response at low frequency region is inevitably affected by enlarging the injection power; therefore, the rising time can only be reduced by  $2.7\text{ ps}$  with the injection power further increasing from  $-9$  to  $-3\text{ dBm}$ . The injection locking can improve the coherence of throughput light. Therefore, the RMS jitter decreases from  $8.17$  to  $7.4\text{ ps}$  with increasing the injection power from  $-12$  to  $-9\text{ dBm}$ , which is attributed to the suppressed phase noise in frequency domain. The BER analyses of the directly modulated and injection-locked WRC-FPLD at 10 Gbit/s with different injection powers over 25-km DSF transmission are compared in Fig. 7(b). In high-speed transmission, the BER performance is significantly affected by the chirp and the modulation bandwidth. Due to the serious dynamic

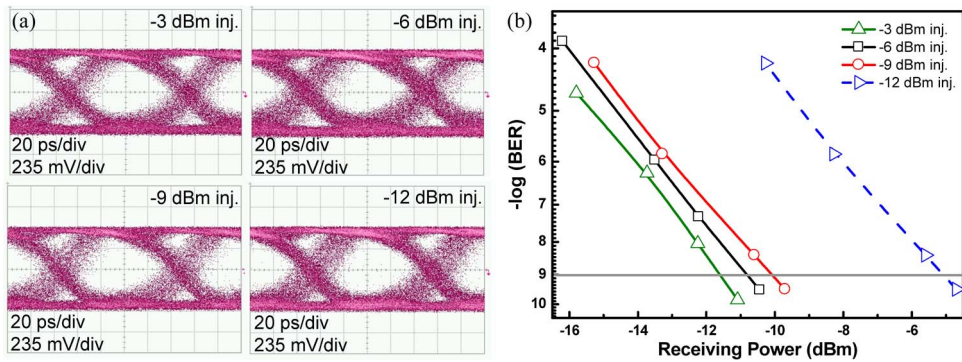


Fig. 7. (a) Measured eye-diagrams and (b) BER responses of the directly modulated and injection-locked WRC-FPLD output after 25-km DSF transmission.

chirp, the injection-locked WRC-FPLD at an injection power of  $-12 \text{ dBm}$  is difficult to reach the required BER of  $10^{-9}$ . By increasing the injection power, the BER performance is significantly improved owing to the enhanced modulation bandwidth and the suppressed dynamic chirp. The power penalty is up to  $-5.1 \text{ dB}$  as the injection power is enlarged from  $-12$  to  $-9 \text{ dBm}$ . With enlarging the injection power to  $-3 \text{ dBm}$ , the receiving power sensitivity of the injection-locked colorless WRC-FPLD output after 25-km DSF transmission is decreased to  $-11.6 \text{ dBm}$  at a BER of  $10^{-9}$ .

To meet the forward error correction (FEC) required BER of  $3.8 \times 10^{-3}$ , the needed SNRs for binary phase-shift keying (BPSK), 4-quadrature-amplitude-modulation (4-QAM), 16-QAM, and 64-QAM orthogonal frequency division multiplexing (OFDM) data are 3.94 dB, 8.54 dB, 15.19 dB, and 21.12 dB, respectively. In view of these criteria, the observed SNR of 6.18 (referred to 7.1 dB) for the injection-locked WRC-FPLD delivered 10-Gbit/s NRZ-OOK which covers a full bandwidth of 7 GHz can only allow the BPSK OFDM transmission. Nevertheless, the usable data format may be extended to m-QAM OFDM as the injection-locked WRC-FPLD could provide a higher SNR within a narrower bandwidth. Typically, the modulation bandwidth of a conventional TO-56-can packaged laser diode is limited at 4 GHz, and the beyond bandwidth operation of 7 GHz in our work has already exceeded over the upper limitation for such a device. If the used bandwidth of the M-QAM OFDM data is slightly narrowed down to 4 GHz or below, the QAM-level can possibly be increased to 64 at least.

#### 4. Conclusion

Based on the modified rate equations, the frequency response of the injection-locked WRC-FPLD is simulated and analyzed. At free-running condition, the WRC-FPLD with lower front-facet reflectance possesses not only broader gain spectrum but also larger modulation bandwidth under a fixed bias current ratio ( $I_{\text{bias}}/I_h$ ) operation when comparing with that with higher front-facet reflectance. Implementing an appropriate amount of injection power, the relaxation oscillation frequency can be enhanced with a decreased damping rate owing to the additional coupling of photon density to the phase for the injection-locked WRC-FPLD. The overly injected and un-modulated photons are unable to create more stimulated emitting photons but become noise component in the cavity of slave laser. In addition, we successfully demonstrate a coherently injection-locked and beyond bandwidth modulated WRC-FPLD-based DWDM-PON system with a data rate of up to 10 Gbit/s. In spite of the limited frequency bandwidth set by the conventional TO-56-can package, the directly modulated WRC-FPLD can be operated for carrying the 10 Gbit/s NRZ-OOK data with ER and SNR of 6.95 dB and 6.18, respectively. In the back-to-back transmission case, the receiving power sensitivity for the  $-3 \text{ dB}$  injection case at a BER of  $10^{-9}$  is  $-15.4 \text{ dBm}$ . After 25-km DSF transmission, the receiving power sensitivity slightly degrades to  $-11.6 \text{ dBm}$  at the same BER of  $10^{-9}$ .

## References

- [1] U. Hilbk, T. Hermes, J. Saniter, and F.-J. Westphal, "High capacity WDM overlay on a passive optical network," *Electron. Lett.*, vol. 32, no. 23, pp. 2162–2163, Nov. 1996.
- [2] D. Gutierrez *et al.*, "Next generation optical access networks," *J. Lightw. Technol.*, vol. 25, no. 11, pp. 3428–3442, Nov. 2007.
- [3] T. Y. Kim and S. K. Han, "Reflective SOA-based bidirectional WDM-PON sharing optical source for up/downlink data and broadcasting transmission," *IEEE Photon. Technol. Lett.*, vol. 18, no. 22, pp. 2350–2352, Nov. 2006.
- [4] S. Y. Kim, S. B. Jun, Y. Takushima, E. S. Son, and Y. C. Chung, "Enhanced performance of RSOA-based WDM PON by using Manchester coding," *J. Opt. Commun. Netw.*, vol. 6, no. 6, pp. 624–630, Jun. 2007.
- [5] H. D. Kim, S. G. Kang, and C. H. Lee, "A low-cost WDM source with an ASE injected Fabry-Pérot semiconductor laser," *IEEE Photon. Technol. Lett.*, vol. 12, no. 8, pp. 1067–1069, Aug. 2000.
- [6] H.-C. Ji, I. Yamashita, and K.-I. Kitayama, "Cost-effective colorless WDM-PON delivering up/down-stream data and broadcast services on a single wavelength using mutually injected Fabry-Pérot laser diodes," *Opt. Exp.*, vol. 16, no. 7, pp. 4520–4528, Mar. 2008.
- [7] Y.-C. Lin, G.-H. Peng, and G.-R. Lin, "Compression of 200 GHz DWDM channelized TDM pulsed carrier from optically mode-locking WRC-FPLD fiber ring at 10 GHz," *Opt. Exp.*, vol. 17, no. 7, pp. 5526–5532, Mar. 2009.
- [8] G.-R. Lin, T.-K. Cheng, Y.-H. Lin, G.-C. Lin, and H.-L. Wang, "A weak-resonant-cavity Fabry-Pérot laser diode with injection-locking mode number-dependent transmission and noise performances," *J. Lightw. Technol.*, vol. 28, no. 9, pp. 1349–1355, May 2010.
- [9] K. Iwatsuki, J. Kani, H. Suzuki, and M. Fujiwara, "Access and metro networks based on WDM technologies," *J. Lightw. Technol.*, vol. 22, no. 11, pp. 2623–2630, Nov. 2004.
- [10] Z. Wu *et al.*, "High-speed WDM-PON using CW injection-locked Fabry-Pérot laser diodes," *Opt. Exp.*, vol. 15, no. 6, pp. 2953–2962, Mar. 2007.
- [11] Z. Al-Qazwini and H. Kim, "Symmetric 10-Gb/s WDM-PON using directly modulated lasers for downlink and RSOAs for uplink," *J. Lightw. Technol.*, vol. 30, no. 12, pp. 1891–1899, Apr. 2012.
- [12] M. Omella, V. Polo, J. Lazaro, B. Schrenk, and J. Prat, "10 Gb/s RSOA transmission by direct duobinary modulation," in *Proc. ECOC*, Sep. 2008, pp. 1–2.
- [13] G.-R. Lin, T.-K. Cheng, G.-C. Lin, and H.-L. Wang, "Suppressing chirp and power penalty of channelized ASE injection-locked mode-number tunable weak-resonant-cavity FPLD transmitter," *IEEE J. Quantum Electron.*, vol. 45, no. 9, pp. 1106–1113, Sep. 2009.
- [14] S.-Y. Lin *et al.*, "Coherent injection-locking of long-cavity colorless laser diodes with low front-facet reflectance for DWDM-PON transmission," *IEEE J. Sel. Top. Quantum Electron.*, vol. 19, no. 4, Jul./Aug. 2013, Art. ID. 1501011.
- [15] R. Lang, "Injection locking properties of a semiconductor laser," *IEEE J. Quantum Electron.*, vol. 18, no. 6, pp. 976–983, Jun. 1982.
- [16] T. B. Simpson, I. M. Liu, and A. Gavrielides, "Bandwidth enhancement and broadband noise reduction in injection-locked semiconductor lasers," *IEEE Photon. Technol. Lett.*, vol. 7, no. 7, pp. 709–711, Jul. 1995.
- [17] E. K. Lau, H.-K. Sung, and M. C. Wu, "Frequency response enhancement of optical injection-locked lasers," *IEEE J. Quantum Electron.*, vol. 44, no. 1, pp. 90–98, Jan. 2008.
- [18] S. Mohrdiek, H. Burkhard, and H. Walter, "Chirp reduction of directly modulated semiconductor lasers at 10 Gb/s by strong CW light injection," *J. Lightw. Technol.*, vol. 12, no. 3, pp. 418–424, Mar. 1994.
- [19] G. Yabre, "Effect of relatively strong light injection on the chirp-to-power ratio and the 3 dB bandwidth of directly modulated semiconductor lasers," *J. Lightw. Technol.*, vol. 14, no. 10, pp. 2367–2373, Oct. 1996.
- [20] E. K. Lau, L. J. Wong, M. C. Wu, "Enhanced modulation characteristics of optical injection-locked lasers: A tutorial," *IEEE J. Sel. Top. Quantum Electron.*, vol. 15, no. 3, pp. 618–633, May/Jun. 2009.
- [21] J. Wang, M. K. Haldar, L. Li, and F. V. C. Mendis, "Enhancement of modulation bandwidth of laser diodes by injection locking," *IEEE Photon. Technol. Lett.*, vol. 8, no. 1, pp. 34–36, Jan. 1996.
- [22] L. Li, "Static and dynamic properties of injection-locked semiconductor lasers," *IEEE J. Quantum Electron.*, vol. 30, no. 8, pp. 1701–1708, Aug. 1994.
- [23] K.-Y. Park, S.-G. Mun, K.-M. Choi, and C.-H. Lee, "A theoretical model of a wavelength-locked Fabry-Pérot laser diode to the externally injected narrow-band ASE," *IEEE Photon. Technol. Lett.*, vol. 17, no. 9, pp. 797–799, Sep. 2005.
- [24] C. H. Henry, N. A. Olsson, and N. K. Dutta, "Locking range and stability of injection locked 1.54  $\mu\text{m}$  InGaAsP semiconductor lasers," *IEEE J. Quantum Electron.*, vol. QE-21, no. 8, pp. 1152–1156, Aug. 1985.
- [25] T. B. Simpson, J. M. Liu, K. F. Huang, and K. Tai, "Nonlinear dynamics induced by external optical injection in semiconductor lasers," *Quantum Semiclassical Opt.*, vol. 9, no. 5, pp. 765–784, Oct. 1997.
- [26] V. Annovazzi-Lodi, A. Scire, M. Sorel, and S. Donati, "Dynamic behavior and locking of a semiconductor laser subjected to external injection," *IEEE J. Quantum Electron.*, vol. 34, no. 12, pp. 2350–2357, Dec. 1998.